Surface Aerodynamic Temperature Modeling over Rainfed Cotton

J. L. Chávez, T. A. Howell, P. H. Gowda, K. S. Copeland, J. H. Prueger

Abstract. *Evapotranspiration (ET) or latent heat flux (LE) can be spatially estimated as an energy balance (EB) residual for land surfaces using remote sensing inputs. The EB equation requires the estimation of net radiation (R_n), soil heat flux (G), and sensible heat flux (H). R_n and G can be estimated with an acceptable accuracy. In computing H, radiometric surface temperature (T_s) is often used instead of surface aerodynamic temperature (T_o), as T_o is neither measured nor easily estimated. This may cause an underestimation of ET because H will be overestimated as T_s is typically larger than T_o for unstable atmospheric conditions. The objectives of this study were to (1) model T_o to improve the estimation of H and consequently ET for advective environments in the semi-arid Texas High Plains, and (2) assess the accuracy of the T_o model using three different methods (aerodynamic profile, lysimeter, and eddy covariance). A 6.5 m tower platform was used to measure profiles of wind speed, air temperature, and relative humidity in and above cotton canopy near a large weighing lysimeter managed under rainfed conditions at the USDA-ARS Conservation and Production Research Laboratory, Bushland, Texas. The T_o was modeled using H as a residual from the EB at the lysimeter location. Results indicated that T_o was better modeled as a linear function of T_s, air temperature, and surface aerodynamic resistance. Modeled T_o showed a very small estimation error (0.1% mean bias error and 3.8% root mean square error) when compared to T_o values measured using the aerodynamic profile data. Even though excellent results were found in this study, the model is only valid for dryland cotton with a leaf area index ranging from 0.2 to 1.3 m^2 m^{-2}. Furthermore, more research is needed to expand the T_o model to cover cotton grown under irrigated conditions and showing larger crop percent cover and leaf area index values, and under different environmental and atmospheric conditions.*

Keywords. *Air temperature, Evapotranspiration, Radiometric surface temperature, Sensible heat flux.*

Due to increase in the world population, food and fiber production under irrigation and rainfed conditions needs to become more efficient and have greater harmony with the environment. Remote sensing (RS) systems and techniques can be employed potentially to assist in irrigation management decisions (Chávez et al., 2009a). For instance, RS can be used to monitor spatially distributed crop water use, as an aid in scheduling irrigations, in general hydrologic models (Gowda et al., 2008), in water rights monitoring (Allen et al., 2004), and to assess overall irrigation project efficiency (Bastiaanssen et al., 2005). Remote sensing of surface energy balance (EB, eq. 1) for land provides instantaneous estimates of latent heat flux (*LE*) or evapotranspiration (ET_i):

$$R_n = G + H + LE \tag{1}$$

where R_n is net radiation, G is the soil heat flux, and H is sensible heat flux, all in units of W m^{-2}, with R_n positive toward the crop surface and G positive into the soil. The other terms (i.e., *LE* and *H*) are positive away from the surface.

The EB equation requires estimation of R_n, G, and H. The values of R_n and G can be estimated with an acceptable accuracy. There are several RS algorithms available in the literature (Gowda et al., 2008) to estimate these non-linearly related EB variables. In most of these models, H is estimated using the radiometric surface temperature (T_s, K). However, H may be overestimated when T_s is used rather than the surface aerodynamic temperature (T_o, K) in the aerodynamic resistance equation (eq. 2). The overestimation of H may occur because T_s is typically larger than T_o. In computing H, most researchers (e.g., Elhaddad and Garcia, 2008; Allen et al., 2007; Kustas and Norman, 2000; Bastiaanssen et al., 1998) use T_s instead of T_o, as T_o is neither measured nor easily estimated. The sensible heat flux is expressed according to the following bulk resistance equation as:

$$H = \rho_a \, Cp_a \, (T_o - T_a) / r_{ah} \tag{2}$$

where ρ_a is air density (kg m^{-3}), Cp_a is specific heat of dry air (approx. 1,005 J kg^{-1} K^{-1}), T_a is average air temperature (K), T_o is the average surface aerodynamic temperature (K),

Submitted for review in December 2009 as manuscript number SW 8360; approved for publication by the Soil & Water Division of ASABE in June 2010.

The mention of trade names of commercial products in this article is solely for the purpose of providing specific information and does not imply recommendation or endorsement by the USDA or Colorado State University

The authors are **José Luis Chávez, ASABE Member Engineer,** Assistant Professor, Department of Civil and Environmental Engineering, Colorado State University, Fort Collins, Colorado; **Terry A. Howell, ASABE Fellow,** Acting Laboratory Director and Research Leader, **Prasanna H. Gowda, ASABE Member Engineer,** Agricultural Engineer, and **Karen S. Copeland,** Soil Scientist, USDA-ARS Conservation and Production Research Laboratory, Soil and Water Management Research Unit, Bushland, Texas; and **John H. Prueger,** Soil Scientist, USDA-ARS National Soil Tilth Laboratory, Soil Water and Air Resources Research Unit, Ames, Iowa. **Corresponding author:** José L. Chávez, Department of Civil and Environmental Engineering, Colorado State University, 1372 Campus Delivery, Fort Collins, CO 80523-1372; phone: 970-491-6095; fax: 970-491-7727; e-mail: jose.chavez@colostate.edu.

which is defined as the temperature at the height of the zero plane displacement (d, m) plus the roughness length for sensible heat transfer (Z_{oh}, m), and r_{ah} is the surface aerodynamic resistance (s m^{-1}) to heat transfer from $d+Z_{oh}$ to Z (horizontal wind speed measurement height, m).

Surface aerodynamic temperature is not measured but calculated. Wenbin et al. (2004) indicated that for homogeneous and isothermal surfaces the definition of aerodynamic and thermodynamic (canopy or surface radiometric, T_s) temperatures are equivalent, but over heterogeneous surfaces there are differences between T_o and T_s. This difference leads to errors in the estimation of H, which in turn leads to errors in the estimation of LE and ET through equation 1. Along those lines, Choudbury et al. (1986), Kustas and Norman (1996), Chehbouni et al. (1997a), Alves et al. (2000), Nagar et al. (2002), Crago et al. (2004), and Yaoming et al. (2003) reported similar findings. They showed differences between T_o and T_s ranging from less than 2°C to 3°C for uniform canopy covers to 10°C to 15°C for partial surface vegetation cover. To account for those differences, many researchers (as indicated below) have parameterized the H equation (eq. 2) in order to use T_s instead of T_o, using different approaches.

Kustas et al. (1989) and Kustas and Norman (1996) increased the surface aerodynamic resistance by adding an extra term that adjusts the surface roughness length for heat transfer. This term expresses the extra resistance that the heat flow encounters above the vegetation canopy in relation to the momentum flux. Bastiaanssen et al. (1998, 2005) circumvented the difficulty in obtaining T_o values by replacing the difference (T_o - T_a) with a dT term in equation 2, derived from cold and hot (extreme) pixels found in the remote sensing/satellite imagery (Landsat 5 and 7). Bastiaanssen et al. (1998) calibrated dT linearly as a function of T_s in a surface energy balance algorithm called SEBAL (Surface Energy Balance Algorithm for Land). Bastiaanssen and Bandara (2001) indicated that SEBAL was only applicable for conditions with wet and dry surfaces, cloudless skies, and flat terrain. Chehbouni et al. (1996, 1997b) introduced a β parameter as a function of leaf area index (LAI, m^2 m^{-2}) in an exponential relationship in the H equation to adjust for the differences between T_o and T_s. Mahrt and Vickers (2004) modeled T_o in terms of T_s, solar radiation (R_s), and vegetation index and considering horizontal wind speed (u) and soil water content. Similarly, Chávez et al. (2005) successfully regressed T_o linearly against T_s, T_a, LAI, and u for corn and soybean crops located near Ames, Iowa.

Crago (1998) and Crago et al. (2004) used RS estimates of LAI and T_s in conjunction with field data to evaluate T_o. Troufleau et al. (1997) added a $-dT$ term to the H equation (eq. 2) with dT being linearly calibrated to the difference (T_o - T_a). Chehbouni et al. (2001) used a combination of dual-angle observations of T_s and a two-layer model to estimate convective surface sensible heat fluxes over sparse grassland. Their model adds a $-dT$ term to the H equation (eq. 2) as Troufleau et al. (1997) did, but dT was related linearly to the difference between nadir and oblique radiometric temperatures (ΔT). Norman et al. (2000) used radiometric surface temperature in a dual-temperature-difference method to minimize measurement errors, obtaining satisfactory estimates of H. In an experiment over homogeneous senescent grass, Sun (1999) found that T_o was linearly related to T_s. He found a very strong correlation and similar coefficients as Huband and Monteith (1986) reported for wheat. Sun (1999) also reported that T_o and T_s were related to T_a within the grass and were approximately linearly correlated over the homogeneous grass except when the wind was weak (i.e., low wind speeds). Sun (1999) concluded that it was more practical to relate T_o to T_s than to find the thermal roughness height (which changes during the day) to estimate H using the bulk resistance equation (eq. 2).

Therefore, the objectives of this study were twofold: (1) to model T_o for dryland cotton under the environmental conditions encountered in the semi-arid U.S. Southern High Plains using radiometric surface temperature and other weather and crop inputs, and (2) to assess the accuracy of the developed cotton T_o model using three independent instruments (i.e., a large monolithic weighing lysimeter, an eddy covariance energy balance system, and a aerodynamic profile tower).

Material and Methods

This section details the location of the experiment, the equipment and methods used to measure surface aerodynamic temperature, the method followed to model T_o for the cotton surface, and a brief description of the statistical methods used in the study.

Study Area

This study was conducted at the USDA-ARS Conservation and Production Research Laboratory (CPRL), located in Bushland, Texas. The geographic coordinates of the CPRL are 35° 11′ N, 102° 06′ W, and its elevation is 1,170 m above mean sea level. Soils at the study site are classified as slowly permeable Pullman clay loam with nearly level to gently sloping fields. The major crops in the region are corn, sorghum, winter wheat, and cotton. Average long-term (30 years) annual precipitation is about 482 mm in the study area. On average, 670 mm of water are needed to grow cotton in this region. However, during the 2008 cotton growing season, there was only 325 mm of rainfall (i.e., just 86.6% of the long-term normal amount expected and only 48.51% of the total amount needed). In the case of air temperature, on average, monthly values were about 2°C lower than normal values, with the exception of the month of July when temperatures were on average 0.8°C warmer. Weather data for the months representing the period of study were obtained from the Texas High Plains Evapotranspiration Network (TXHPET, 2008), while long-term data were from TXCLB (2009). In addition, for the period May-October 2008, average monthly wind speed, relative humidity, and solar irradiance were 4.22 m s^{-1}, 59.03%, and 22.83 MJ m^{-2} d^{-1}, respectively.

Weighing Lysimeter Data

A soil-water mass balance using data from a large precision monolithic weighing lysimeter located at the USDA-ARS, CPRL provided ET data. The lysimeter (3 m long × 3 m wide × 2.4 m deep) was situated in the middle of the 2.4 ha cotton field that was managed under dryland conditions (no irrigation after emergence). The lysimeter was equipped with one net radiometer (Q*7.1, Radiation and Energy Balance Systems [REBS], Bellevue, Wash.) and two infrared thermometers (model IRt/c5, Exergen, Watertown, Mass.) for measuring R_n and T_s, respectively. In addition, the following sensors completed the instrumentation at the lysi-

meter location: four soil heat flux plates (HFT3, REBS, Campbell Scientific, Inc. [CSI], Logan, Utah), four averaging soil temperature thermocouple probes (TCAV-L, CSI, Logan, Utah), an albedometer (CM-14, Kipp & Zonen, Bohemia, N.Y.), and a tipping-bucket rain gauge (model 6011B, Qualimetrics, Inc., Sacramento, Cal.). Details on the calibration and performance of the USDA-Bushland lysimeter can be found in Howell et al. (1995).

Air Temperature and Wind Profiles

An air temperature and horizontal wind (aerodynamic) profile tower was installed in the northeast corner of a rainfed (dryland) cotton field (210 m long × 200 m wide) during the 2008 cotton growing season. The location of the tower in the field was selected considering the predominant wind direction (from southwest). This location provided an approximate fetch of 250 m along the predominant upwind direction.

The tower was composed of six cross-arms, each holding one horizontal wind speed sensor (model 03101 R.M. Young Wind Sentry, CSI, Logan, Utah) and one air temperature and relative humidity sensor (model HMP45C, Vaisala, Inc., CSI, Logan, Utah). Additionally, one solar radiation sensor or pyranometer (model LI200X, Li-Cor, Inc., CSI, Logan, Utah) was installed on the second arm, and two infrared thermometers (model IRt/c5, Exergen, Watertown, Mass.) were installed on the third arm. In the ground, two soil heat flux plates (model HFT3, REBS, CSI, Logan, Utah), four soil temperature probes (model 107, CSI, Logan, Utah), and two time domain reflectometer (TDR) soil water content probes (model CS-616, CSI, Logan, Utah) were installed. The heights of each set of sensors (temperature and wind) mounted on the cross-arms were 0.57, 1.57, 2.57, 3.57, 4.57, and 6.43 m from the ground surface, respectively.

Data collected during the months of June, July, August, and the beginning of September were used in the study. Initially, daytime data (values when R_n was larger than 50 W m^{-2}) were analyzed. Later, the analyzed data included only those values within 2 h of solar noon. This last criterion was chosen because most RS overpasses (both satellite and airborne) occurred close to noon. In addition, rainy days were excluded from the analysis. There were six rainy days in June (18-21, 24, and 28), seven in July (3, 8-10, 15, 28, and 29), nine in August (11-14, 16-19, and 29), and one on September 3. Thus, the number of 15 min observations, around noon (local standard time), used in the T_o modeling was 985. For the evaluation component of the study, nine independent days (DOY) were selected: June 22 (174), June 30 (182), July 16 (198), July 20 (202), July 30 (212), August 8 (221), August 15 (228), September 1 (245), and September 7 (251). The rationale followed in the selection of these evaluation days was to have enough days (at least two per month) to span the range of environmental conditions encountered throughout the experiment duration. These days were chosen at random from the pool of non-previously excluded days within a month.

The methodology found in Arya (2001) was followed to obtain T_o using the data collected with the aerodynamic profile tower. Briefly, first the Monin-Obukhov (M-O) stability length (L, m) (Foken, 2006; Liu et al., 2007) was obtained from the slope of plotting Z_m vs. the Richardson number (R_i). The Richardson number is used to describe the atmospheric stability conditions ($R_i < 0$ for unstable conditions). The Richardson number quantifies the mixing efficiency influence of air buoyancy and wind shear on turbulent heat transfer (Arya, 2001), and it is defined as:

$$R_i = \frac{g}{T_a}\left[\frac{\partial\theta}{\partial z}\Big/\left(\frac{\partial u}{\partial z}\right)^2\right] \tag{3}$$

where T_a is air temperature, g is acceleration of gravity, θ is potential temperature, z is height above ground, and u is wind speed. If temperature gradients ($\partial T_a / \partial z$) are measured close to the surface, they can replace $\partial\theta / \partial z$ with little error in estimating R_i.

Practically, Z_m/L is equal to R_i. Z_m is the geometric mean height (m) of the heights between two consecutive T_a and u measurement levels. It is calculated as $(Z_i \times Z_{i+1})^{0.5}$, where Z_i is a given measurement height level (from the ground, m) and Z_{i+1} is the subsequent measurement height level. R_i was obtained using the difference in T_a and u between consecutive measurement (profile tower cross-arms) height levels (Z_i and Z_{i+1}), Z_i, Z_{i+1}, and Z_m. Second, a plot of $\ln(Z_i) - \Psi_m(Z_i/L)$ vs. u_i is graphed, and from the slope of the curve the fraction k/u_* was obtained, where k is the von Kármán constant (0.41), u_* is the friction velocity (m s^{-1}), and $\Psi_m(Z/L)$ was the atmospheric stability factor for momentum transfer. Third, a plot of $\ln(Z_i) - \Psi_h(Z_i/L)$ vs. T_{ai} was graphed, and from the slope of the curve the fraction k/T_* was obtained, where $\Psi_h(Z/L)$ is the atmospheric stability factor for heat transfer, and T_* is the air temperature scaling factor (K). We used T_{ai} in our graph instead of the potential temperature (θ, K), which is the appropriate temperature to be used in the graph because our measurements were close to the surface where these two air temperatures are very similar (i.e., ΔZ was small, hence minimum adiabatic lapse in air temperature). Once T_* was obtained, the surface aerodynamic temperature was computed by means of equation 4. T_o was computed individually for each height level of the aerodynamic profile tower, using T_{ai} and Z_i values from corresponding levels, and the results were averaged to find the averaged T_o value for a particular day in the study:

$$T_o = T_a - \left(\frac{T_*}{k}\right)\times\left[\ln\left(\frac{Z}{Z_o}\right) - \Psi_h\left(\frac{Z}{L}\right)\right] \tag{4}$$

where Z_o is the roughness length (m) of shear forces, above the zero plane displacement (d, m), where the mean horizontal wind speed will go to zero as a result of flow obstacle (momentum sink). Z_o was obtained, following Arya (2001), from the ordinate intercept $\ln(Z_o)$ of the plot of $\ln(Z_i) - \Psi_m(Z_i/L)$ vs. u_i.

Eddy Covariance Data

An eddy covariance (EC) energy balance system was installed on the north side of the southwest lysimeter field, about 100 m north of the lysimeter and about 220 m from the south border of the southwest cotton field; thus, good fetch was guaranteed for the predominant south-southwest direction winds. This EC system was installed as a part of the 2008 Bushland Evapotranspiration and Agricultural Remote Sensing Experiment (BEAREX08) to better understand the energy balance closure problem associated with EC systems. The EC system consisted of a fast-response 3D sonic anemometer (model CSAT3, CSI, Logan, Utah), a fast-response open-path infrared gas (H_2O and CO_2) analyzer

(model LI-7500, Li-Cor, Inc., Lincoln, Neb.), an air temperature and relative humidity sensor (model HMP45C, Vaisala Inc., Woburn, Mass.), and a measurement and control system and datalogger (model CR5000, CSI, Logan, Utah). The instrumentation also included one net radiometer (model CNR1, Kipp & Zonen, Bohemia, N.Y.), three soil heat flux plates (model HFP01SC, Hukseflux, CSI, Logan, Utah), six soil temperature probes (model 107-L, CSI, Logan, Utah), two infrared thermometers (model SI-111, Apogee, Logan, Utah), and a tipping-bucket rain gauge (model TB4, CSI, Logan, Utah).

The EC CSAT3 and LI-7500 sensors measured air temperature, wind speed, water vapor, and CO_2 concentrations at a frequency of 20 Hz (20 samples per second). From these raw data, 15 min averages of *LE* and *H* fluxes were computed by the EC program and datalogger system. The EC system was installed at a 2.0 m height above ground level and kept at the same height during the entire length of the experiment. The cotton canopy height varied from 0.10 m by early June to about 0.60 m by early August of 2008. The CSAT3 sensor was oriented toward the predominant wind direction, with an azimuth angle of approximately 225° from north.

The raw high-frequency data (20 samples per second) were corrected for effects of density fluctuations induced by heat fluxes on the measurement of eddy fluxes of water vapor using the LI-7500. This correction is called the WPL (Webb, Pearman, and Leuning) correction (Webb et al., 1980). Leuning (2007) provides a detailed description of the principles and theory of the WPL correction.

In addition, adjustments for lack of energy balance closure on *LE* and *H* were provided by means of the Bowen ratio (BR) procedure. Details on the procedure can be found in Chávez et al. (2009a).

Modeling Surface Aerodynamic Temperature

The T_o was modeled as a function of T_s, T_a, LAI, u, and/or r_{ah} using multiple linear regression procedures similar to those reported by Chávez et al. (2005) and Mahrt and Vickers (2004). However, in our case, "measured or inverted" T_o was derived from the 15 min data on ET, R_n, and G measured at the lysimeter location, solving equation 1 for H as a residual, and by inverting equation 2 and solving for T_o. All variables involved in the regression were obtained at the lysimeter location. The aerodynamic resistance (r_{ah}) was calculated using equation 5 (the derivation of this equation can be found in the Appendix) considering the atmospheric stability condition (mostly unstable) and following an iterative procedure outlined by Chávez et al. (2005):

$$r_{ah} = \frac{\ln\left(\frac{Z-d}{Z_{oh}}\right) - \psi_h\left(\frac{Z-d}{L}\right) + \psi_h\left(\frac{Z_{oh}}{L}\right)}{u_* k} \quad (5)$$

LAI values were estimated using equation 6 from Chávez et al. (2009b). Estimates of LAI were performed for those days where surface reflectance data were obtained using an EXOTECH handheld radiometer, which emulates the wavelengths of Landsat 5 and 7 blue, green, red, and NIR spectral bands. In addition, estimated LAI values were verified by measured LAI values collected on July 18 and 28 and on August 7:

$$\text{LAI} = 0.263e^{(3.813\ \text{OSAVI})} \quad (6)$$

where OSAVI is the optimized soil adjusted vegetation index (Rondeaux et al., 1996):

$$\text{OSAVI} = \frac{1.16(\text{NIR} - \text{R})}{(\text{NIR} + \text{R} + 0.016)} \quad (7)$$

where NIR and R are reflectance (fraction) in the near-infrared and red bands of the electromagnetic spectrum, respectively. NIR and R were measured with the EXOTECH radiometer.

Daily cotton LAI (LAI_d) values were obtained by fitting a sigmoid curve to measured and estimated LAI values as a function of the day of year (DOY), as shown in equation 8:

$$\text{LAI}_d = 0.492 + \frac{0.8774}{1 + e^{-\left(\frac{\text{DOY}-208.41}{4.928}\right)}} \quad (8)$$

Equation 8 resulted with a goodness of fit (R^2) of 0.987 and a root mean square error (RMSE) of 0.025 $m^2\ m^{-2}$. LAI ranged from about 0.2 to 1.3 $m^2\ m^{-2}$ during the days considered in this study.

Statistical Analysis

The accuracy of the newly developed cotton T_o model was assessed by comparing modeled T_o with T_o inverted from the different evaluation methods (i.e., lysimeter, aerodynamic profile, and eddy covariance). The comparison analysis included the least square linear regression coefficients (slope and intercept), goodness of fit (R^2), mean bias error (MBE), and root mean square error (RMSE). The MBE and RMSE were calculated following the procedures of Willmott (1982).

Results and Discussion

Aerodynamic Temperature Development Analysis

After deriving T_o values from the lysimeter data, the first analysis (table 1) indicated that T_o was strongly and positively correlated to T_s, showing a correlation factor of 0.71. In addition, T_o was correlated to T_a (factor of 0.6) and weakly and negatively correlated to LAI (-0.10) and u (-0.21) when using the daytime values. Table 1 shows correlation values for T_a and u values from level 3 of the aerodynamic tower (2.57 m height).

The best multiple linear regression model for the dataset collected within 2 h of solar noon (n = 985) resulted in equation 9, with a goodness of fit (R^2) of 0.7. The T_o for this equation was called $T_{o\ (1)}$. The T_a and u values were both taken from the third cross-arm sensor level:

$$T_{o(1)} = 0.57T_s + 0.14T_a + 0.81\text{LAI} - 0.97u + 14.9 \quad (9)$$

However, when correlating T_o to r_{ah} the correlation factor was 0.47, i.e., much higher than the corresponding factors for

Table 1. Correlation of T_o with T_s, T_a, LAI, and u using day time values.

	T_o	T_s	T_{a3}	LAI	u_3
T_o	1				
T_s	0.71	1			
T_{a3}	0.60	0.88	1		
LAI	-0.10	-0.30	-0.16	1	
u_3	-0.21	0.14	0.20	-0.41	1

Table 2. Statistical analysis of modeled T_o using measured T_o by three systems.

Statistic	Aerodynamic Profile		Lysimeter		Eddy Covariance	
	$T_{o(1)}$	$T_{o(2)}$	$T_{o(1)}$	$T_{o(2)}$	$T_{o(1)}$	$T_{o(2)}$
a	0.631	1.145	0.809	1.298	0.425	0.943
b	14.422	-4.226	10.383	-7.783	21.803	2.398
R^2	0.631	0.982	0.743	0.969	0.355	0.858
MBE (°C)	3.95	0.16	4.74	1.00	4.32	0.67
RMSE (°C)	2.95	1.02	2.18	1.61	4.49	2.14
MBE (%)	14.25	0.13	17.03	2.83	16.33	2.24
RMSE (%)	10.95	3.77	8.66	5.67	15.37	6.53

[a] a = regression equation slope, b = ordinate intercept, R^2 = goodness of fit, MBE = mean bias error, and RMSE = root mean square error.

LAI and u. Therefore, an improved regression model was found when T_o was fit to T_s, T_a, and r_{ah} with a larger goodness of fit (R^2) of 0.76 (eq. 10). This result must be due to the fact that r_{ah} was a better representation than LAI and u separately of the non-linear mechanism that integrates surface roughness, wind friction/shear, atmospheric stability conditions (L), and plant characteristics, e.g., crop canopy height (h_c, m):

$$T_{o(2)} = 0.5T_s + 0.5T_a + 0.15r_{ah} - 1.4 \quad (10)$$

It is anticipated that better results will be obtained once data from stable and unstable atmospheric conditions are separated and analyzed individually (two models). Some days (or parts of the day, mostly afternoons) presented stable atmospheric conditions when H was negative because T_s was smaller than T_o.

Aerodynamic Temperature Model Evaluation

The profile method used to determine T_o is depicted in the upper graph of figure 1, where R_i is plotted vs. Z_m for the nine days used for the model evaluation. The Richardson number was negative for all nine days, which indicated the unstable condition of the atmosphere. In addition, R_i became less negative (approaching zero) as the cotton season progressed. As the cotton grew and shaded the ground, and due to some soil moisture from rainfall, the sensible heat flux rate decreased; thus, T_a was closer to T_o in magnitude toward the

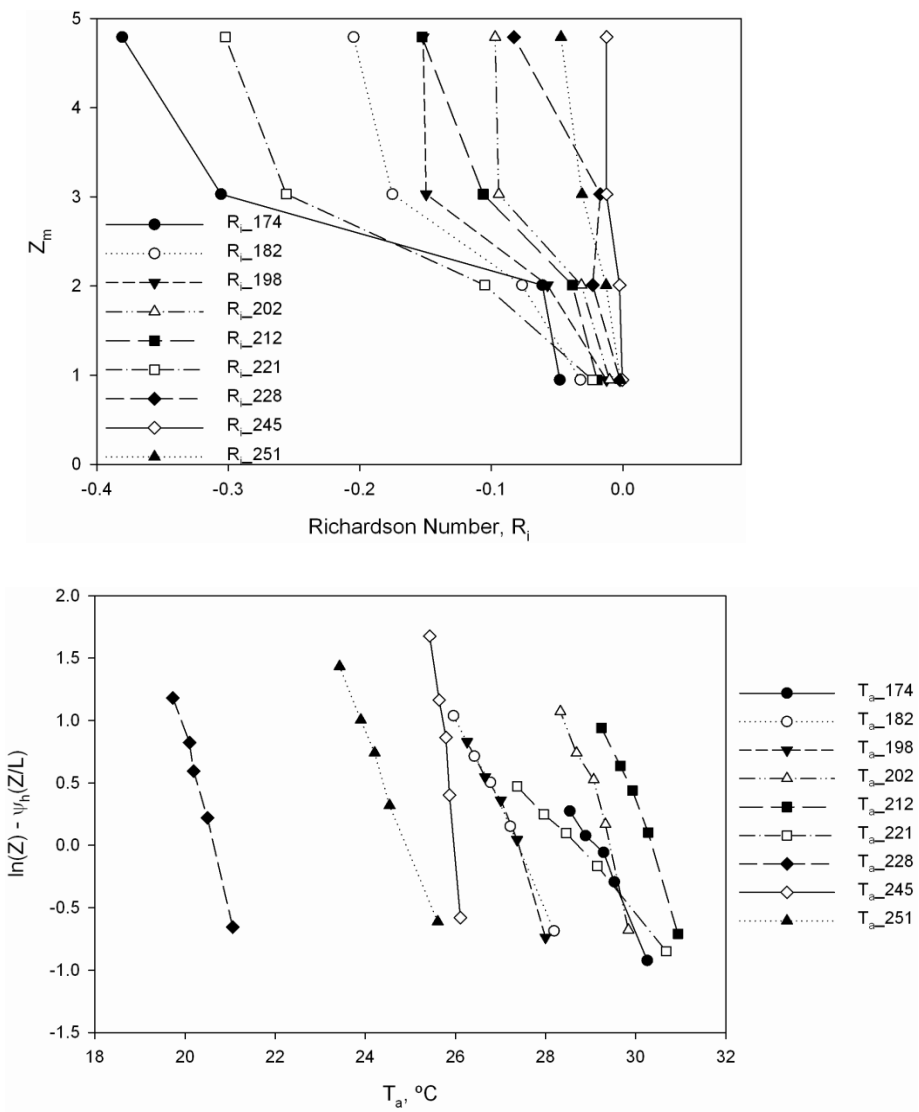

Figure 1. (upper graph) Profile method Richardson number vs. Z_m used to obtain the M-O stability length (L, m), and (lower graph) method used for T_* determination.

end of the cropping season. This is also evident in the lower graph of figure 1, where T_a values are lower for larger DOY numbers. By drawing a best-fit straight line through these points, one obtains the slope k/T_*. This fraction (inverted) was used in equation 4 to compute T_o for this aerodynamic profile method.

The resulting T_o values from the profile method as well as from the lysimeter and eddy covariance systems are graphed in figures 2a, 2b, and 2c, respectively. The plots of modeled ($T_{o(i)}$) vs. measured T_o by the different methods, mentioned above, show a much better fit to the 1:1 line (thick diagonal black line) of model $T_{o(2)}$, i.e., to the model that is a function of T_s, T_a, and r_{ah}.

One reason for the better performance of $T_{o(2)}$ over $T_{o(1)}$ may be due to the fact that in equation 9 the LAI varied over a narrow range, and equation 9 did not incorporate the roughness effect on wind speed in conjunction with corrections for atmospheric stability conditions, as was the case with equation 10.

In terms of the quantification of the performance of modeled T_o, table 2 details the following: linear regression coefficients (modeled $T_o = a \times$ measured $T_o + b$), linear regression goodness of fit (R^2), and MBE and RMSE both in units of temperature (°C) and percent (%).

Model $T_{o(2)}$ resulted with the largest R^2 (i.e., 0.98, 0.97, and 0.86 respectively) for all three evaluating methods. On average, T_o was modeled with an error range of 0.1°C to 1.0°C and a error standard deviation of approximately 1°C to 2°C (i.e., MBE and RMSE of 0.13% to 2.8% and 3.8% to 6.5%, respectively), which is a low error. It was observed that T_o values from all three evaluating methods were remarkably close. There was less agreement for modeled T_o with T_o determined with the eddy covariance EB system. We attribute this difference to the lack of energy balance closure under sparse vegetation or dry surface conditions. In general, the EC EB closure ranged from 60.1% to 101.5%, with an overall average of 77.1% and standard deviation of 14.6%. In addition, it was noticed that there was no or poor correlation between T_o and radiometric surface temperature and air temperature when horizontal wind speeds were lower than 1 m s^{-1}, indicating a possible decoupling of the surface and atmosphere due to lack of sufficient turbulence (eddies). This could have been a limitation for the EC system, since it is well known (Chávez et al., 2009a) that the EC system flux measurements are based on the premise of existing atmospheric turbulence. Hence, a lack of eddies when slow wind speeds are present would signify poor flux measurements. Nevertheless, the EC system seems to have been able to satisfactorily measure the Bowen ratio (BR = H/LE) used in the lack of EB closure correction or adjustments performed.

The results found in this study present strong evidence that the T_o model based on T_s, T_a, and r_{ah} (eq. 10) is a robust model that can be used in the estimation of surface aerodynamic temperature for dryland cotton, for which LAI ranged from about 0.2 to 1.3 m^2 m^{-2}.

In terms of practical applicability of the results found in this study, the reader may pose the question: "What would the implication of the study be on ET?" Chávez and Neale (2003) performed an error analysis (uncertainty) on the different terms of the energy balance of equation 1. In particular, their study indicated that using the radiometric surface temperature (T_s) instead of the appropriate surface aero-

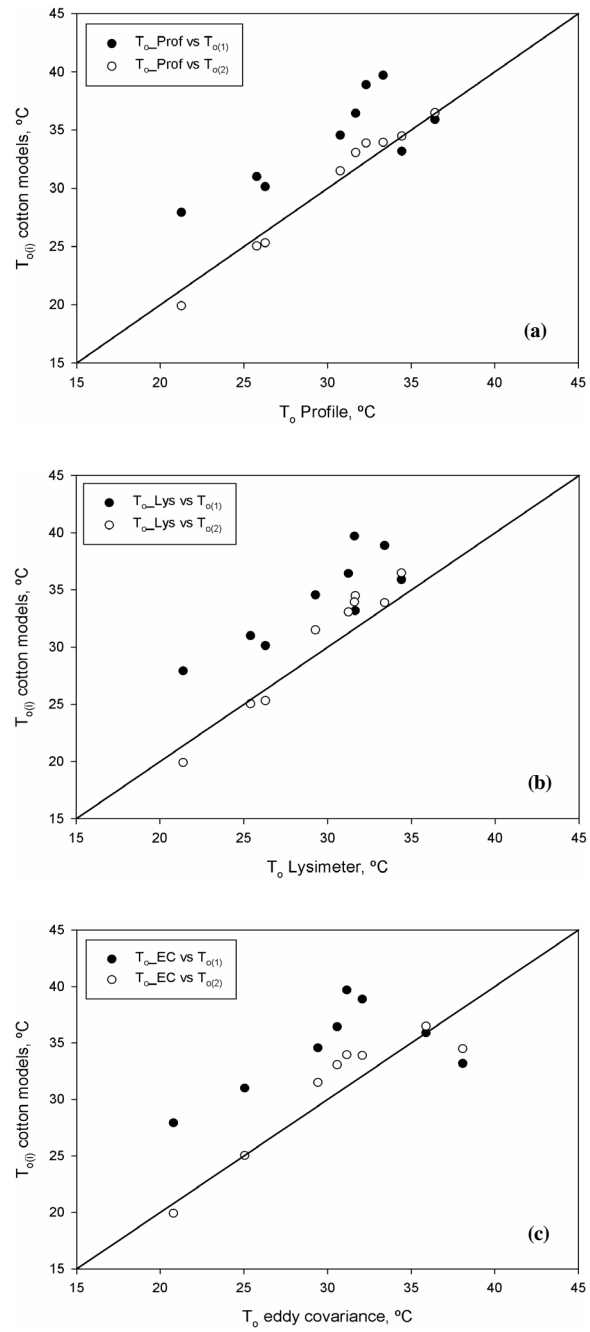

Figure 2. $T_{o(i)}$ modeled vs. measured T_o using (a) profile method, (b) lysimeter, and (c) eddy covariance.

dynamic temperature (T_o) resulted in an estimation error of the sensible heat flux (H) of -5.2 ±151 W m^{-2}, or in percent approximately -17% ±50% (error range of -67% to 33%); which is a large error. The error in H propagated to the calculation of latent heat flux, which resulted in an estimation error of -32 ±150 W m^{-2}, or an underestimation of 6.4% ±30% (error range of -36.4% to 23.6%). Hence, for the extreme case of overestimation of H ($T_s > T_o$, common case under unstable atmospheric conditions), the use of the radiometric surface temperature instead of the aerodynamic temperature resulted in an H error of 33% and therefore in an underestimation of ET by 36.4%. Therefore, with this method (H calculated using T_s instead of T_o), 36.4% less

water would have been applied to the crop, which would have experienced a reduction in yield.

In contrast, in the current study the largest verified error in the estimation of the surface aerodynamic temperature (therefore in H) was 2.8% ±6.5% (i.e., error range of -3.7% to 9.3%). This small error in H would result in an estimation error in LE (or ET) ranging approximately from -1% to +3%, provided that R_n, G, and r_{ah} were well estimated. Thus, the underestimation of 3.7% in H would mean an overestimation of ET of 3% (in this study). Consequently, there could be a potential improvement in the estimation of ET of approximately 20.6% (i.e., 23.6% to 3%). In this case, this 20.6% improvement in the estimation of actual ET (removal of the underestimation of ET) translates into an increment of irrigation (consumptive use only without accounting for precipitation, irrigation system efficiencies, or the need for salts lixiviation fraction) of 138 mm (5.4 in.) when modeled T_o is used instead of T_s in the estimation of sensible heat flux during the seasonal cotton growth period in the Texas High Plains.

Conclusion

Remote sensing algorithms are capable of estimating crop evapotranspiration (ET). To improve spatial estimation of ET, sensible heat flux needs to be estimated more accurately through the parameterization of surface aerodynamic temperature (T_o). In this study, T_o was modeled as a function of radiometric surface temperature, air temperature, leaf area index, horizontal wind speed, and surface aerodynamic resistance using T_o derived from lysimetric data and multiple linear regression. Evaluation of modeled T_o using independent data and T_o derived from the profile, lysimeter, and eddy covariance methods indicated that T_o model based on T_s, T_a, and r_{ah} (eq. 10) is a robust model that can be used in the estimation of surface aerodynamic temperature for dryland cotton, for which LAI ranged from about 0.2 to 1.3 m^2 m^{-2}.

Validation of modeled T_o using remote sensing inputs (T_s and LAI) and validation for cotton grown under irrigated conditions and larger crop cover and LAI values, under different environmental and atmospheric conditions, needs to be performed for a generalization and transferability of the developed T_o model.

Acknowledgements

This study was possible thanks to funding provided through the Ogallala Aquifer Program and the USDA-ARS. Our sincere appreciation to the following individuals who provided assistance: technicians, Dr. Susan O'Shaughnessy, Thomas Clarke, Dr. Doug Hunsaker, and a number of student workers from the CPRL. We also want to express our sincere gratitude to the anonymous reviewers who provided key comments that improved the quality of the manuscript.

References

Allen, R. G., M. Tasumi, A. Morse, and R. Trezza. 2004. A Landsat-based energy balance and evapotranspiration model in western U.S. water rights regulation and planning. *Irrig. and Drain. Sys*. 19(3-4): 251-268.

Allen, R. G., M. Tasumi, and R. Trezza. 2007. Satellite-based energy balance for mapping evapotranspiration with internalized calibration (METRIC): Model. *ASCE J. Irrig. and Drain. Eng.* 133(4): 380-394.

Alves, I., J. C. Fontes, and L. S. Pereira. 2000. Evapotranspiration estimation from infrared surface temperature: I. The performance of the flux equation. *Trans. ASAE* 43(3): 591-598.

Arya, S. P. 2001. *Introduction to Micrometeorology.* 2nd ed. San Diego, Cal.: Academic Press.

Bastiaanssen, W. G. M., and K. M. P. S. Bandara. 2001. Evaporative depletion assessments for irrigated watersheds in Sri Lanka. *Irrig. Sci.* 21(1): 1-15.

Bastiaanssen, W. G. M., M. Menenti, R. A. Feddes, and A. A. M. Holtslag. 1998. A remote sensing surface energy balance algorithm for Land (SEBAL), Part 1: Formulation. *J. Hydrol.* 212-213: 198-212.

Bastiaanssen, W. G. M., E. J. M. Noordman, H. Pelgrum, G. Davids, B. P. Thoreson, and R. G. Allen. 2005. SEBAL model with remotely sensed data to improve water-resources management under actual field conditions. *J. Irrig Drainage Eng*. 131(1): 85-93.

Brutsaert, W. 1975. On a derivable formula for long-wave radiation from clear skies. *Water Resour. Res*. 11(5): 742-744.

Brutsaert, W. 1982. *Evaporation into the Atmosphere. Theory, History, and Applications*. Boston, Mass.: D. Reidel.

Brutsaert, W. H., and H. S. Stricker. 1979. An advection-aridity approach to estimate actual regional evapotranspiration. *Water Resour. Res*. 15(2): 443-450.

Businger, J. A. 1988. A note on the Businger-Dyer profiles. *Boundary-Layer Meteorol*. 42(1-2): 145-151

Chávez, J. L., and C. M. U. Neale. 2003. Validating airborne multispectral remotely sensed heat fluxes with ground energy balance tower and heat flux source area (footprint) functions. ASAE-CIGR Meeting Paper No. 033128. St. Joseph, Mich.: ASAE.

Chávez, J. L., C. M. U. Neale, L. E. Hipps, J. H. Prueger, and W. P. Kustas. 2005. Comparing aircraft-based remotely sensed energy balance fluxes with eddy covariance tower data using heat flux source area functions. *J. Hydromet.* 6(6): 923-940.

Chávez, J. L., T. A. Howell, and K. S. Copeland. 2009a. Evaluating eddy covariance cotton ET measurements in a semiarid advective environment with large weighing lysimeters. *Irrig. Sci*. 28(1): 35-50.

Chávez, J. L., P. H. Gowda, T. A. Howell, C. M. U. Neale, and K. S. Copeland. 2009b. Estimating hourly crop ET using a two-source energy balance model and multispectral airborne imagery. *Irrig. Sci*. 28(1): 79-91.

Chehbouni, A., D. Lo Seen, E. G. Njoku, and B. M. Monteny. 1996. Examination of the difference between radiative and aerodynamic surface temperature over sparsely vegetated surfaces. *Remote Sensing Environ*. 58(2): 177-186.

Chehbouni, A., R. L. Scott, D. C. Goodrich, J. P. Lhomme, J. Qi, and Y. H. Kerr. 1997a. Examination of the relationship between radiative and aerodynamic surface temperature over patchy surfaces. Available at: www.tucson.ars.ag.gov/salsa/archive/publications/ams_preprints/chehbouni2.PDF Accessed 15 November 2009.

Chehbouni, A., J. Qi, D. Lo Seen, Y. H. Kerr, G. Dedieu, S. Moran, M. Daubas, and B. M. Monteny. 1997b. Estimation of real evapotranspiration. In *Proc. Intl. Workshop on Remote Sensing and Water Resources.* Rome, Italy: United Nations FAO. Available at: www.fao.org/docrep/W7320B/w7320b29.htm. Accessed 15 November 2009.

Chehbouni, A, Y. Nouvellon, J. P. Lhomme, C. Watts, G. Boulet, Y. H. Kerr, M. S. Moran, and D .C. Goodrich. 2001. Estimation of surface sensible heat flux using dual-angle observations of radiative surface temperature. *Agric. Forest Meteorol*. 108(1): 55-65.

Choudhury, B. J., R. J. Reginato, and S. B. Idso. 1986. An analysis of infrared temperature observations over wheat and calculation of latent heat flux. *Agric. Forest Meteorol*. 37(1): 75-88.
Crago, R. D. 1998. Radiometric and equivalent isothermal surface temperatures. *Water Resour. Res*. 34(11): 3017-3023.
Crago, R., M. Friedl, W. Kustas, and Y. Wang. 2004. Investigation of aerodynamic and radiometric land surface temperatures. *NASA Scientific and Technical Aerospace Reports* (*STAR*) 42(21): 201.
Dyer, A. J. 1974. A review of flux-profile relationships. *Boundary-Layer Meteorol*. 7(3): 363-372.
Dyer, A. J., and B. B. Hicks. 1970. Flux-gradient relationship in the constant flux layer. *Quart. J. Royal Meteorol. Soc*. 96(410): 715-721.
Elhaddad, A., and L. A. Garcia. 2008. Surface energy balance-based model for estimating evapotranspiration taking into account spatial variability in weather. *ASCE J. Irrig. and Drain. Engr.* 134(6): 681-689.
Foken, T. 2006. 50 Years of the Monin-Obukhov similarity theory. *Boundary-Layer Meteorol*. 119(3): 431-447.
Garratt, J. R., and B. B. Hicks. 1973. Momentum, heat and vapour transfer to and from natural and artificial surfaces. *Quart. J. Royal Meteorol. Soc*. 99(422): 680-687.
Gowda, P. H., J. L. Chavez, P. D. Colaizzi, S. R. Evett, T. A. Howell, and J. A. Tolk. 2008. ET mapping for agricultural water management: Present status and challenges. *Irrig. Sci*. 26(3): 223-237.
Howell, T. A., A. D. Schneider, D. A. Dusek, T. H. Marek, and J. L. Steiner. 1995. Calibration and scale performance of Bushland weighing lysimeters. *Trans. ASAE* 38(4): 1019-1024.
Huband, N. D. S., and J. L. Monteith. 1986. Radiative surface temperature and energy balance of a wheat canopy. *Boundary-Layer Meteorol.* 36(1-2): 1-17.
Kustas, W. P., and J. M. Norman. 1996. Use of remote sensing for evapotranspiration monitoring over land surfaces. *Hydrol. Sci.* 41(4): 495-516.
Kustas, W. P., and J. M. Norman. 2000. A two-source energy balance approach using bidirectional radiometric temperature observations for sparse canopy covered surfaces. *Agron. J*. 92(5): 847-854.
Kustas, W. P., B. J. Choudhury, M. S. Moran, R. J. Reginato, and R. D. Jackson. 1989. Determination of sensible heat flux over sparse canopy using thermal infrared data. *Agric. Forest Meteorol*. 44(3-4): 197-216.
Leuning, R. 2007. The correct form of the Webb, Pearman, and Leuning equation for eddy fluxes of trace gases in steady and non-steady, horizontal homogeneous flow. *Boundary-Layer Meteorol*. 123(2): 263-267.
Liu, S., L. Lu, D. Mao, and L. Jia. 2007. Evaluating parameterizations of aerodynamic resistance to heat transfer using field measurements. *Hydrol. Earth System Sci.* 11(2): 769-783.
Mahrt, L., and D. Vickers. 2004. Bulk formulation of the surface heat flux. *Boundary-Layer Meteorol.* 110(3): 357-379.
Nagar, S. G., P. Seetaramayya, A. Tyagi, and S. S. Sing. 2002. Estimation of daytime surface fluxes of radiation and heat at Anand during 13-17 May 1997. *Current Sci*. 83(1): 39-46.
Norman, J. M., W. P. Kustas, J. H. Prueger, and G. R. Diak. 2000. Surface flux estimation using radiometric temperature: A dual-temperature-difference method to minimize measurement errors. *Water Resour. Res*. 36(8): 2263-2274.
Paulson, C. A. 1970. The mathematical representation of wind speed and temperature profiles in the unstable atmospheric surface layer. *J. Appl. Meteorol*. 9(6): 857-861
Rondeaux, G., M. Steven, and F. Baret. 1996. Optimization of soil-adjusted vegetation indices. *Remote Sensing Environ*. 55(2): 97-107.
Sugita. M., and W. Brutsaert. 1990. Regional surface fluxes from remotely sensed surface skin temperature and lower boundary layer measurements. *Water Resour. Res*. 26(12): 2937-2944.
Sun, J. 1999. Diurnal variations of thermal roughness height over a grassland. *Boundary-Layer Meteorol*. 92(3): 407-427.
Troufleau, D., A. Vidal, A. Beaudoin, M. S. Moran, M. A. Weltz, D. C. Goodrich, J. Washburne, and A. F. Rahman. 1997. Optical-microwave synergy for estimating surface sensible heat flux over a semi-arid rangeland. *Remote Sensing Rev.* 15: 113-132.
TXCLB. 2009. Texas normals, means, and extremes. College Station, Tex.: Texas A&M University, Department of Atmospheric Sciences. Available at: http://atmo.tamu.edu/osc/norm/. Accessed 5 November 2009.
TXHPET. 2008. Daily weather data. College Station, Tex.: Texas A&M University, Texas High Plains Evapotranspiration Network. Available at: http://txhighplainset.tamu.edu/weather_options.jsp. Accessed 20 December 2008.
Webb, E. K. 1970. Profile relationships: The log-linear range, and extension to strong stability. *Quart. J. Royal Meteorol. Soc*. 96(407): 67-90.
Webb, E. K., G. I. Pearman, and R. Leuning. 1980. Correction of flux measurements for density effects due to heat and water vapour transfer. *Quart. J. Royal Meteorol. Soc*. 106(447): 85-100.
Wenbin, M., C. Zhongming, S. Linsheng, G. Wenliang, L. Xiuling, Y. Tingrong, P. Jan, H. Guanglun, and Y. Xiurong. 2004. A scheme for pixel-scale aerodynamic surface temperature over hilly land. *Adv. Atmos. Sci*. 21(1): 125-131.
Willmott, C. J. 1982. Some comments on the evaluation of model performance. *Bull. American Meteorol. Soc*. 63(11): 1309-1313.
Yang, K., N. Tamai, and T. Krike. 2001. Analytical solution of the surface layer similarity equations. *J. Appl. Meteorol*. 40(9): 1647-1653.
Yaoming, M., W. Jiemin, H. Ronghui, W. Guoan, M. Menenti, S. Zhongo, H. Zeyong, G. Feng, and W. Jun. 2003. Remote sensing parameterization of land surface heat fluxes over arid and semi-arid areas. *Adv. Atmos. Sci*. 20(4): 530-539.

Appendix

Derivation of the Surface Aerodynamic Resistance Equation (Eq. 5)

The surface aerodynamic resistance (r_{ah}, s m^{-1}) for heat transfer is typically written, in its simplest form for neutral atmospheric conditions (adiabatic conditions or no heat exchange), as:

$$r_{ah} = \frac{\ln\left(\dfrac{Z-d}{Z_{oh}}\right)}{u_* k} \tag{11}$$

where Z is the height (m) from the ground at which the wind speed and air temperature were measured. The zero-plane displacement height is d (m), Z_{oh} is the roughness length (m) for heat transfer, k is the von Kármán constant (0.41) for turbulent diffusion, and u_* (m s^{-1}) is the friction velocity.

Friction velocity for neutral atmospheric conditions is expressed as:

$$u_* = \frac{u\,k}{\ln\left(\dfrac{Z-d}{Z_{om}}\right)} \tag{12}$$

where u is the horizontal wind speed (m s^{-1}), and Z_{om} is the roughness length (m) for momentum transfer.

In the equations presented above, Z_{oh}, Z_{om}, and d can be estimated from the crop canopy height (h_c, m) measurements according to Brutsaert's (1975, 1982) procedure:

$$Z_{om} = 0.123 \times h_c \tag{13}$$

$$Z_{oh} = 0.1 \times Z_{om} \tag{14}$$

$$d = 0.67 \times h_c \tag{15}$$

Substituting equation 12 into equation 11, we obtain equation 16, which is a more commonly use equation for neutral conditions, according to Garratt and Hicks (1973) and Brutsaert and Stricker (1979):

$$r_{ah} = \frac{\ln\left(\frac{Z-d}{Z_{oh}}\right)\ln\left(\frac{Z-d}{Z_{om}}\right)}{u\,k^2} \tag{16}$$

To account for buoyancy forces, from the surface to the atmosphere above, one must adjust equation 16 based on the Monin-Obukhov surface layer similarity theory, as shown by Brutsaert (1982):

$$r_{ah} = \left\{\left[\ln\left(\frac{Z-d}{Z_{oh}}\right) - \psi_h\left(\frac{Z-d}{L}\right)\right] \times \left[\ln\left(\frac{Z-d}{Z_{om}}\right) - \psi_m\left(\frac{Z-d}{L}\right)\right]\right\} \div u\,k^2 \tag{17}$$

where $\psi_h[(Z - d)/L]$ and $\psi_m[(Z - d)/L]$ are stability correction functions for heat and sensible momentum transfer, respectively. In equation 17, L is the Monin-Obukhov stability length (m) (Foken, 2006; Liu et al., 2007):

$$L = (u_*)^3\, T_a\, C_{pa} \,/\, (g\, k\, H) \tag{18}$$

where g is gravity acceleration. The stability correction factor (or functions) for atmospheric heat transfer and momentum transfer, for unstable conditions ($L < 0$), can be determined by Businger-Dyer formulations (Dyer and Hicks, 1970; Dyer, 1974; Businger, 1988; Sugita and Brutsaert, 1990):

$$\Psi_h\left(\frac{Z-d}{L}\right) = 2\ln\left(\frac{1-x^2}{2}\right) \tag{19}$$

$$\Psi_m\left(\frac{Z-d}{L}\right) = 2\ln\left(\frac{1-x}{2}\right) + \ln\left(\frac{1-x^2}{2}\right) - 2\arctan(x) + \left(\frac{\pi}{2}\right) \tag{20}$$

$$x = 1 - \left[16\left(\frac{Z-d}{L}\right)\right]^{0.25} \tag{21}$$

For stable atmospheric conditions ($L > 0$), Webb (1970) suggested:

$$\Psi_m\left(\frac{Z-d}{L}\right) = \Psi_h\left(\frac{Z-d}{L}\right) = -5\left(\frac{Z-d}{L}\right) \tag{22}$$

Furthermore, equation 17 can be completed to account for the effects of roughness heights for momentum and heat transfer, as indicated in equation 23 (Paulson, 1970; Yang et al., 2001; Liu et al., 2007):

$$r_{ah} = \left\{\left[\ln\left(\frac{Z-d}{Z_{oh}}\right) - \psi_h\left(\frac{Z-d}{L}\right) + \psi_h\left(\frac{Z_{oh}}{L}\right)\right] \times \left[\ln\left(\frac{Z-d}{Z_{om}}\right) - \psi_m\left(\frac{Z-d}{L}\right) + \psi_m\left(\frac{Z_{om}}{L}\right)\right]\right\} \div u\,k^2 \tag{23}$$

Many researchers use equation 17 instead of equation 23 due to the fact that the $\psi_m(Z_{om}/L)$ and $\psi_m(Z_{oh}/L)$ terms are very small.

Similarly, friction velocity (eq. 12) is adjusted for atmospheric stability using the Monin-Obukhov similarity theory as:

$$u_* = \frac{u\,k}{\ln\left(\frac{Z-d}{Z_{om}}\right) - \psi_m\left(\frac{Z-d}{L}\right) + \psi_m\left(\frac{Z_{om}}{L}\right)} \tag{24}$$

Then, re-arranging equation 24, solving for u, and substituting u into equation 23 yields:

$$r_{ah} = \frac{\ln\left(\frac{Z-d}{Z_{oh}}\right) - \psi_h\left(\frac{Z-d}{L}\right) + \psi_h\left(\frac{Z_{oh}}{L}\right)}{u_*\,k} \tag{25}$$

This resulting equation (eq. 25) is the equation presented in the body of the article (eq. 5) and as applied by Chávez et al. (2005).